

Non-additivity of decoherence rates in superconducting qubits

Guido Burkard¹ and Frederico Brito^{2,1}

¹IBM T. J. Watson Research Center, P. O. Box 218, Yorktown Heights, NY 10598, USA

²Departamento de Física da Materia Condensada, Instituto de Física Gleb Wataghin, Universidade Estadual de Campinas, Campinas-SP 13083-970, Brazil

We show that the relaxation and decoherence rates T_1^{-1} and T_2^{-1} of a qubit coupled to several noise sources are in general not additive, i.e., that the total rates are not the sums of the rates due to each individual noise source. To demonstrate this, we calculate the relaxation and pure dephasing rates T_1^{-1} and T_2^{-1} of a superconducting (SC) qubit in the Born-Markov approximation in the presence of several circuit impedances Z_i using network graph theory and determine their deviation from additivity (the mixing term). We find that there is no mixing term in T_1^{-1} and that the mixing terms in T_1^{-1} and T_2^{-1} can be positive or negative, leading to reduced or enhanced relaxation and decoherence times T_1 and T_2 . The mixing term due to the circuit inductance L at the qubit transition frequency ω_{01} is generally of second order in $\omega_{01}L=Z_i$, but of third order if all impedances Z_i are pure resistances. We calculate $T_{1,2}$ for an example of a SC qubit coupled to two impedances.

Introduction. The loss of quantum coherence and the transition from quantum to classical behavior has been a long-standing fundamental problem [1, 2]. More recently, the phenomenon of decoherence has attracted much interest in a new context, because quantum coherence is an essential prerequisite for quantum computation. For some systems that have been proposed as physical realizations of quantum hardware (see, e.g., Ref. 3), there have been extensive studies, both in theory and experiment, of the mechanisms that are causing decoherence. Generally, an open quantum system loses coherence by interacting with a large number of external degrees of freedom (heat bath, environment). It is the physical nature of the environment and the system-environment coupling that distinguishes the various mechanisms of decoherence. It is quite natural that for a given open quantum system there will be several distinct decoherence mechanisms. Previous studies have typically tried to identify the strongest source of decoherence, i.e., the one that leads to the shortest relaxation and decoherence times, T_1 and T_2 , and to analyze the corresponding mechanism in order to predict decoherence times. In the presence of several decoherence sources for the same system, the decoherence rates T_1^{-1} and T_2^{-1} have usually been quoted separately for each source. Often, it is assumed that the total decoherence or relaxation rate is the sum of the rates corresponding to the various sources (see, e.g., Ref. 4 for the case of superconducting qubits). In the theory of electron scattering in metals, this assumption is also known as Matthiessen's rule [5]. In this paper, we show that the total decoherence and relaxation rates of a quantum system in the presence of several decoherence sources are not necessarily the sums of the rates due to each of the mechanisms separately, and that the corrections to additivity (mixing terms) can have both signs.

We investigate the decoherence due to several sources in superconducting (SC) qubits [6, 7, 8, 9, 10, 11] (see Ref. 4 for a review of SC qubits); the general idea of the present analysis may however be applied to other systems as well. SC qubits are small SC circuits that

contain Josephson junctions. The differences φ_i of the SC phases across the junctions J_i , where $i=1;\dots;n$, are the relevant quantum degrees of freedom of the system; we denote the quantum operator of these phase differences collectively with the vector $\varphi = (\varphi_1; \varphi_2; \dots; \varphi_n)$. The circuit is constructed such that it gives rise to a potential $U(\varphi)$ which forms a double well and therefore can be used to encode one qubit. In our analysis, we will make use of a recently developed circuit theory describing the dissipative dynamics of arbitrary SC qubits [12]. Our analysis relies on the theory for open quantum systems introduced by Caldeira and Leggett [1] where the dissipative elements (impedances Z_i) are represented by a set of baths of harmonic oscillators (an alternative approach to a quantum theory of dissipative electric circuits is to represent impedances as infinite transmission lines [13]).

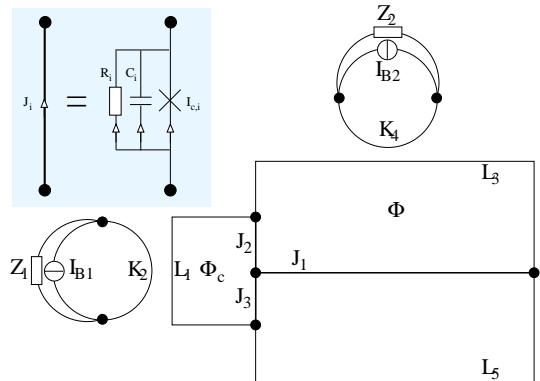


FIG. 1: Circuit graph of the gradiometer qubit [14], under the influence of noise from two sources Z_1 and Z_2 . Branches of the graph denote Josephson junctions J_i , inductances L_i and K_i , current sources I_{B_i} , and external impedances Z_i , and are connected by the nodes (black dots) of the graph. Inset: A resistively-shunted Josephson junction (RSJ) J_1 , represented by a thick line in the circuit graph, is modeled by an ideal junction (cross) with critical current I_{c1} , shunt resistance R_1 , and junction capacitance C_1 .

For concreteness, we demonstrate our theory on the example of the gradiometer qubit with $n = 3$ junctions that is currently under experimental investigation [14], see Fig. 1. We emphasize, however, that our findings are completely general and apply to arbitrary SC flux qubits. The qubit is controlled by applying a magnetic flux Φ to the small loop on the left by driving a current I_{B1} in a coil next to it, and simultaneously by applying a magnetic flux Φ on one side of the gradiometer using I_{B2} . Real current sources are not ideal, i.e., they are characterized by a finite frequency-dependent impedance $Z_i(\omega)$, giving rise to decoherence of the qubit [15, 16, 17, 18]. Since the shunt resistances R_i of the junctions are typically much larger ($\gg M$) than the impedances of the current sources (between 50 and 10 k Ω), we concentrate in our example on the impedances Z_1 and Z_2 of the two current sources.

Using circuit graph theory [12], we obtain the classical equations of motion of a general SC circuit in the form

$$C' \dot{\Phi} = \frac{\partial U}{\partial \Phi} - M \dot{\mathbf{x}}; \quad (1)$$

where C is the $n \times n$ capacitance matrix and $U(\Phi; I_{B1}; I_{B2})$ is the potential. The dissipation matrix $M(t)$ is a real, symmetric, and causal $n \times n$ matrix, i.e., $M(t)^T = M(t)$ for all t , and $M(t) = 0$ for $t < 0$. The convolution is defined as $(f \otimes g)(t) = \int_{-\infty}^t f(t-t')g(t')dt'$. Since it is not explicitly used here, we will not further specify U . The dissipation matrix in the Fourier representation [19], $M(\omega) = \int_{-\infty}^{\infty} e^{i\omega t} M(t) dt$, where $\gamma > 0$ has been introduced to ensure convergence (at the end, $\gamma \rightarrow 0$), can be found from circuit theory [12] as

$$M(\omega) = m L_Z(\omega)^{-1} m^T; \quad (2)$$

where m denotes a real $n \times n_Z$ matrix that can be obtained from the circuit inductances, and where the $n_Z \times n_Z$ matrix $L_Z(\omega)$ has the form

$$L_Z(\omega) = L_Z(\omega) + L_C; \quad (3)$$

Here, n_Z is the number of impedances in the circuit (in our example, $n_Z = 2$) and $L_Z(\omega) = Z(\omega) = i\omega Z$, where $Z(\omega)$ the impedance matrix. The frequency-independent and real inductance matrix L_C can be obtained from the circuit inductances [12]. Since we start from independent impedances, Z and L_Z are diagonal. Moreover, note that

$$\text{Im} L_Z^{-1} = \omega \text{Re} Z(\omega) + \omega^2 L_C(\omega) (\text{Re} Z(\omega))^{-1} L_C(\omega); \quad (4)$$

where $L_C(\omega) = L_C + \text{Im} Z(\omega) = i\omega Z$, thus it follows from $\text{Re} Z > 0$ that $\text{Im} L_Z^{-1}$ and $\text{Im} M$ are positive matrices.

Multi-dimensional Caldeira-Leggett model. We now construct a Caldeira-Leggett Hamiltonian [1], $H = H_S + H_B + H_{SB}$, that reproduces the classical dissipative equation of motion, Eq. (1), and that is composed of parts for the system (S), for m harmonic oscillator baths (B),

and for the system-bath (SB) coupling,

$$H_S = \frac{1}{2} Q^T C^{-1} Q + \frac{0}{2} U(\Phi); \quad (5)$$

$$H_B = \sum_{j=1}^m \left(\frac{p_j^2}{2m_j} + \frac{1}{2} m_j \omega_j^2 x_j^2 \right); \quad (6)$$

$$H_{SB} = \sum_{j=1}^m c_j x_j; \quad (7)$$

where the capacitor charges Q are the canonically conjugate momenta corresponding to the Josephson fluxes ($\Phi = 2\pi \Phi_0 \mathbf{x}$), where $\mathbf{x} = (x_1; \dots; x_m)$, and c is a real $n \times m$ matrix. From the classical equations of motion of the system and bath coordinates and by taking the Fourier transform, we obtain Eq. (1), with $M(\omega) = (2\pi\omega)^2 c [\mathbf{m}(\omega^2 - \omega_j^2)]^{-1} c^T = M(\omega)^T$, where the $m \times m$ mass and frequency matrices \mathbf{m} and ω_j are diagonal with entries m_j and ω_j . Using the regularization $\omega_j \rightarrow \omega_j + i\gamma$ when taking Fourier transforms also guarantees that $M(\omega)$ is causal and real.

Defining the spectral density of the environment as the matrix function

$$J(\omega) = \frac{1}{2} c \mathbf{m}^{-1} [\omega^2 - \omega_j^2]^{-1} c^T; \quad (8)$$

where $\omega_j(\mathbf{x}) = \omega_j(x_j)$, we find the relation

$$J(\omega) = \frac{0}{2} \text{Im} M(\omega) = \sum_{j=1}^m J_j(\omega) m_j(\omega) m_j(\omega)^T; \quad (9)$$

where we have used the spectral decomposition of the real, positive, and symmetric matrix [19] $\text{Im} M(\omega)$, with the eigenvalues $J_j(\omega) > 0$ and the real and normalized eigenvectors $m_j(\omega)$. The integer m_j ; n_j denotes the maximal rank of $\text{Im} M(\omega)$, i.e., $m_j = \max(\text{rank}[\text{Im} M(\omega)])$. Using Eq. (9), and choosing $c_{ij} = \sum_{j=1}^m m_i(\omega_j)$, we find that $J_j(\omega)$ is the spectral density of the j -th bath of harmonic oscillators in the environment, $J_j(\omega) = \frac{0}{2} \sum_{j=1}^m m_j(\omega) m_j(\omega)^T$.

The master equation of the reduced system density matrix $\rho_S = \text{Tr}_B \rho$ in the Born-Markov approximation, expressed in the eigenbasis $\{ |j\rangle \}$ of H_S , yields the Bloch-Redfield equation [20], $\dot{\rho}_{nm}(t) = -i[\rho_{nm}(t), H_S] - R_{nmkl}(t) \rho_{kl}(t)$, where $R_{nmkl} = \ln \int_0^\infty ds \int_0^\infty ds' \langle H_{SB}(t) H_{SB}(t-s) H_{SB}(t-s') H_{SB}(t-s'-s) \rangle$, and $|j\rangle$ is the eigenenergy of H_S corresponding to the eigenstate $|j\rangle$. The Redfield tensor has the form $R_{nmkl} = \sum_{r, r', r''} \Gamma_{nmkl}^{(+)}$ with the rates $\Gamma_{nmkl}^{(+)} = \int_0^\infty dt \exp(-it|n\rangle \langle n|) \text{Tr}_B H_{SB}(t) \rho_B H_{SB}(0) |m\rangle \langle m|$ and $\Gamma_{knml}^{(+)} = \Gamma_{nmkl}^{(+)}$, where $H_{SB}(t) = \sum_j e^{itH_B} H_{SB} e^{-itH_B} |j\rangle \langle j|$. For the system-bath interaction Hamiltonian, Eq. (7), we obtain

$$\text{Re} \Gamma_{nmkl}^{(+)} = \sum_j \text{Im} J(\omega_j) \Gamma_{nmkl}^{(j)} \frac{e^{-\omega_j |n\rangle \langle n|}}{\sinh(\omega_j |j\rangle \langle j|)}; \quad (10)$$

$$\text{Im} \Gamma_{nmkl}^{(+)} = \frac{2}{P} \sum_0^{Z-1} \frac{\text{Im} J(\omega_j) \Gamma_{nmkl}^{(j)}}{\omega_j^2 \omega_{nk}^2} \omega_j |n\rangle \langle n| \coth \frac{\omega_j}{2};$$

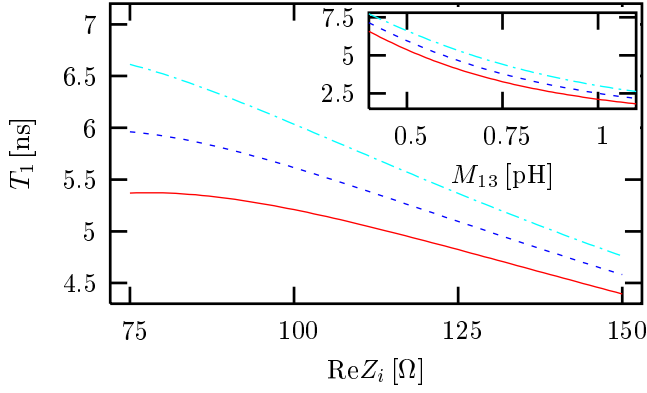


FIG. 2: The relaxation rate T_1 without the mixing term (dashed blue line), and including the mixing term for $R_{sm} = +10k$ (solid red line) and $R_{sm} = -10k$ (dot-dashed light blue line), for $M_{13} = 0.5$ pH as a function of $\text{Re}Z_i$. Inset: T_1 for $R = \text{Re}Z_i = 75$ for a range of mutual inductances M_{13} .

where $'_{nk} = \ln j_{ki}$. For two levels $n = 0, 1$, and within the secular approximation, we can determine the relaxation and decoherence rates T_1^{-1} and T_2^{-1} in the Bloch equation as [12] $T_1^{-1} = 2\text{Re}(\binom{+}{0110} + \binom{+}{1001})$ and $T_2^{-1} = (2T_1)^{-1} + T^{-1}$, where $T^{-1} = \text{Re}(\binom{+}{0000} + \binom{+}{1111} - 2\binom{+}{0011})$ is the pure dephasing rate. Using Eq. (10), we find

$$T_1^{-1} = 4'_{01} \mathcal{J}(!_{01})'_{01} \coth \frac{!_{01}}{2}; \quad (11)$$

$$T^{-1} = \frac{2}{!_{!} 0} \lim_{! \rightarrow 0} ('_{00} \quad '_{11})^y \frac{\mathcal{J}(!)}{!} ('_{00} \quad '_{11}): \quad (12)$$

With the spectral decomposition, Eq. (9), we obtain

$$T_1^{-1} = 4 \sum_{j=1}^{X^n} '_{01} m_j (!_{01})^2 \mathcal{J}_j (!_{01}) \coth \frac{!_{01}}{2}; \quad (13)$$

$$T^{-1} = \frac{2}{!_{!} 0} \sum_{j=1}^{X^n} \ln_j (0) ('_{00} \quad '_{11})^y \frac{\mathcal{J}_j (!)}{!} ('_{00} \quad '_{11}): \quad (14)$$

In the last equation, we have used that the limit $\lim_{! \rightarrow 0} m_j (!) = \lim_{! \rightarrow 0} m_j (!) m_j (!)$ exists because $\ln_j (!) \mathcal{J}_j (!) = 1$ and thus all components of $m_j (!)$ are bounded.

Mixing Terms. In the case where L_c is diagonal, or if its off-diagonal elements can be neglected because they are much smaller than $L_z (!)$ for all frequencies $!$, we find, using Eq. (3), that the contributions due to different impedances Z_i are independent, thus $m = n_z$ and $M (!) = m L_z (!)^{-1} m^T = \sum_{j=1}^m m_j m_j^T i! = (\sum_{j=1}^m Z_j (!) + i! L_{jj})$, where $m_j = m_j$ is simply the j -th column of the matrix m and L_{jj} is the j -th diagonal entry of L_c . As a consequence, the total rates $1=T_1^{-1}$ and $1=T^{-1}$ are the sums of

the individual rates, $1=T_1^{(j)}$ and $1=T^{(j)}$, where

$$\frac{1}{T_1^{(j)}} = 4 \frac{0}{2} \sum_{j=1}^m \mathcal{J}_j (!_{01})^2 \text{Re} \frac{!_{01} \coth (!_{01}=2)}{Z_j (!_{01}) + i!_{01} L_{jj}}; \quad (15)$$

$$\frac{1}{T^{(j)}} = \frac{2}{!_{!} 0} \lim_{! \rightarrow 0} ('_{00} \quad '_{11})^y \frac{\mathcal{J}_j (!)}{!} ('_{00} \quad '_{11}): \quad (16)$$

In general, the situation is more complicated because current fluctuations due to different impedances are mixed by the presence of the circuit. In the regime $L_c \gg L_z (!)$, we can use Eq. (3) to make the expansion

$$L_z^{-1} = L_z^{-1} - L_z^{-1} L_c L_z^{-1} + L_z^{-1} L_c L_z^{-1} L_c L_z^{-1} \quad (17):$$

The series Eq. (17) can be partially resummed,

$$L_z^{-1} (!) = \text{diag} \frac{i!}{Z_j (!) + i! L_{jj}} + L_{mix}^{-1} (!): \quad (18)$$

The first term in Eq. (18) simply gives rise to the sum of the individual rates, as in Eqs. (15) and (16), while the second term gives rise to mixed terms in the total rates. The rates can therefore be decomposed as ($X = 1; 2; \dots$)

$$\frac{1}{T_X} = \sum_j^X \frac{1}{T_X^{(j)}} + \frac{1}{T_X^{(mix)}}: \quad (19)$$

For the mixing term in the relaxation rate, we find

$$\frac{1}{T_1^{(mix)}} = 4 \frac{0}{2} \sum_{j=1}^m '_{01} m_j \text{Im} L_{mix}^{-1} (!_{01}) m_j^T '_{01} \coth \frac{!_{01}}{2}: \quad (20)$$

We can show that there is no mixing term in the pure dephasing rate, i.e., $1=T^{(mix)} = 0$, and consequently, $T_2^{(mix)} = 2T_1^{(mix)}$. The absence of a mixing term in T can be understood as follows. Since the first term in Eq. (17) only contributes to the first term in Eq. (18), the low-frequency asymptotic of $\text{Im} L_{mix}^{-1} (!)^{-1}$ involves only $!^2$ and higher powers of $!$ (it can be assumed that $Z_i (! = 0)$ is finite), thus Eq. (12) yields zero in the limit $! \rightarrow 0$. While $\text{Im} L_z^{-1}$ is a positive matrix, $\text{Im} L_{mix}^{-1}$ does not need to be positive, therefore the mixing term $1=T_1^{(mix)}$ can be both positive or negative. Furthermore, we can show that if $Z (!)$ is real, only odd powers of $! L_c Z^{-1}$ occur, and in particular, that in this case $\text{Im} L_{mix}^{-1} (!)^{-1} = 0 (!^3)$, by using Eq. (4) to write $\mathcal{J} (!) ' ! Z (!)^{-1} !^3 Z (!)^{-1} L_c Z (!)^{-1} L_c Z (!)^{-1}$, up to higher orders in $! L_c Z (!)^{-1}$.

In the case of two external impedances, $n_z = 2$, we can completely resum Eq. (17), with the result

$$L_{m \text{ ix}}^{-1}(\omega) = \frac{L_{12}}{(Z_1(\omega) = i\omega + L_{11})(Z_2(\omega) = i\omega + L_{22})} \quad (21)$$

where L_{ij} are the matrix elements of L_C and where the approximation in Eq. (21) holds up to $O(\omega^{-3})$. In lowest order in $\omega = Z_i$, we find, with $\omega_{12} = (\omega_{01} m_1)(\omega_{01} m_2)$,

$$\frac{1}{T_1^{(m \text{ ix})}} = \frac{\omega^2}{2} \text{Im} \frac{8'_{12} L_{12}}{Z_1(\omega_{01}) Z_2(\omega_{01})} \coth \frac{\omega_{01}}{2}; \quad (22)$$

If $R_i = Z_i(\omega_{01})$ are real (pure resistances) then, as predicted above, the imaginary part of the second-order term in Eq. (21) vanishes, and we resort to third order,

$$\text{Im} L_{m \text{ ix}}^{-1} = \frac{\omega^3 L_{12}}{R_1 R_2} \frac{L_{12}}{R_1} \frac{L_{11} + L_{22}}{R_1 + R_2} \frac{L_{12}}{R_2}; \quad (23)$$

neglecting terms in $O(R_j^{-4})$. If $L_{12} = L_{jj}$, we obtain $\text{Im} L_{m \text{ ix}}^{-1} = (\omega^3 L_{12} = R_1 R_2)(L_{11} = R_1 + L_{22} = R_2) \times$, and

$$\frac{1}{T_1^{(m \text{ ix})}} = \frac{\omega^2}{2} \frac{8'_{01} L_{12}}{R_1 R_2} \frac{L_{11} + L_{22}}{R_1 + R_2} \omega_{12} \coth \frac{\omega_{01}}{2}; \quad (24)$$

For the gradiometer qubit (Fig. 1), we find $L_{12} = M_{12} M_{13} M_{34} = L_1 L_3$, $L_{11} = L_2$, $L_{22} = L_4$, where L_k denotes the self-inductance of branch X_k ($X = L$ or K) and M_{k_1} is the mutual inductance between branches X_k and X_1 , and where we assume $M_{ij} = L_k$. The ratio between the mixing the single-impedance contribution scales as

$$\frac{1 = T_1^{(m \text{ ix})}}{1 = T_1^{(j)}} = \frac{\omega_{01}^2 L_{12} L}{R^2}; \quad (25)$$

where we have assumed $R_1 = R_2 = R$, $L_{11} = L_{22} = L$, and $\omega_{01} m_1 = \omega_{01} m_2$.

We have calculated T_1 at temperature $T = \hbar \omega_{01} = k_B$ for the circuit Fig. 1, for a critical current $I_c = 0.3$ A for all junctions, and for the inductances $L_1 = 30$ pH, $L_3 = 680$ pH, $L_2 = L_4 = 12$ nH, $M_{12} = \frac{1}{2} \sqrt{L_1 L_2}$,

$$\frac{L_{12}}{Z_1(\omega) = i\omega + L_{11}} \frac{1}{1} \frac{L_{12}}{Z_2(\omega) = i\omega + L_{22}} \frac{\omega^2 L_{12}}{Z_1(\omega) Z_2(\omega)} \times; \quad (21)$$

$M_{34} = \frac{1}{2} \sqrt{L_3 L_4}$ (strong inductive coupling), $M_{35} = 6$ pH, with $\omega_{01} = 2 \times 30$ GHz, and with the impedances $Z = R$, $Z_2 = R + iR_{\text{im}}$, where R and $R_{\text{im}} = 10$ k are real ($R_{\text{im}} > 0$ corresponds to an inductive, $R_{\text{im}} < 0$ to a capacitive character of Z_i). In Fig. 2, we plot T_1 with and without mixing for a fixed value of $M_{13} = 0.5$ pH and a range of $R = \text{Re} Z_i$. In the inset of Fig. 2, we plot T_1 (with mixing) and $(T_1^{(1)})^{-1} + (T_1^{(2)})^{-1})^{-1}$ (without mixing) for $R = 75$ for a range of mutual inductances M_{13} ; for this plot, we numerically computed the double minimum of the potential U and ω_{01} for each value of M_{13} . The plots (Fig. 2) clearly show that summing the decoherence rates without taking into account mixing term can both underestimate or overestimate the relaxation rate $1 = T_1$, leading to either an over- or underestimate of the relaxation and decoherence times T_1 and T_2 .

Higher-order terms in the Born series. Two series expansions have been made in our analysis, (i) the Born approximation to lowest order in the parameter $\beta = R_Q = Z_i(\omega_{01}) = \omega_{01} T_1$, where β is a dimensionless ratio of inductances [12] and $R_Q = \hbar/e^2$ is the quantum of resistance, and (ii) the expansion Eq. (17) in the parameter $\omega_{01} L = Z_i$, where L is the inductance of the circuit, where we included higher orders. The question arises whether the terms in the next order in β in the Born approximation could be of comparable magnitude to those taken into account in $1 = T_1^{(m \text{ ix})}$. In our example, we could neglect such terms, because $\beta = \frac{L}{R_Q} = 0.001 = 0.1 \ll 1$, but in cases where $\beta > 1$, higher orders in the Born approximation may have to be taken into account.

Acknowledgments. We thank David Divincenzo and Roger Koch for useful discussions. FB would like to acknowledge the hospitality of the Quantum Condensed Matter Theory group at Boston University. FB is supported by Fundaçao de Amparo a Pesquisa do Estado de São Paulo (FAPESP).

- [1] A. O. Caldeira and A. J. Leggett, Ann. Phys. (N.Y.) 143, 374 (1983).
- [2] W. H. Zurek, Rev. Mod. Phys. 75, 715 (2003).
- [3] Special issue on Experimental proposals for Quantum Computation, Fortsch. Phys. 48 (2000).
- [4] Y. Makhlin, G. Schon, and A. Shnirman, Rev. Mod. Phys. 73, 357 (2001).
- [5] N. W. Ashcroft and N. D. Mermin, Solid state physics (Holt-Saunders, 1983).
- [6] J. E. Mooij, T. P. Orlando, L. Levitov, L. Tian, C. H.

- van der Wal, S. Lloyd, Science 285, 1036 (1999).
- [7] T. P. Orlando, J. E. Mooij, L. Tian, C. H. van der Wal, L. S. Levitov, S. Lloyd, J. J. Mazo, Phys. Rev. B 60, 15398 (1999).
- [8] C. H. van der Wal, A. C. J. ter Haar, F. K. Wilhelm, R. N. Schouten, C. J. P. M. Harmans, T. P. Orlando, S. Lloyd, and J. E. Mooij, Science 290, 773 (2000).
- [9] I. Chiorescu, Y. Nakamura, C. J. P. M. Harmans, J. E. Mooij, Science 299, 1869 (2003).
- [10] J. R. Friedman, V. Patel, W. Chen, S. K. Tolpygo, and

- J. E. Lukens, *Nature* 406, 43 (2000).
- [1] R. Koch, J. Kirtley, J. Rozen, J. Sun, G. Keefe, F. M. Il-
liken, C. Tsuei, D. Di Vincenzo, *Bull. Am. Phys. Soc.* 48,
367 (2003).
- [2] G. Burkard, R. H. Koch, and D. P. Di Vincenzo, *Phys.*
Rev. B 69, 064503 (2004).
- [3] B. Yurke and J. S. Denker, *Phys. Rev. A* 29, 1419 (1984).
- [4] R. Koch et al., unpublished.
- [5] L. Tian, L. S. Levitov, J. E. Mooij, T. P. Orlando, C.
H. van der Wal, S. Lloyd, in *Quantum Mesoscopic Phenom-
ena and Mesoscopic Devices in Microelectronics*, I.
O. Kulik, R. Ellialtıoglu, eds. (Kluwer, Dordrecht, 2000),
pp. 429-438; cond-mat/9910062.
- [6] L. Tian, S. Lloyd, and T. P. Orlando, *Phys. Rev. B* 65,
144516 (2002).
- [7] C. H. van der Wal, F. K. Wilhelm, C. J. P. M. Hamans,
and J. E. Mooij, *Eur. Phys. J. B* 31, 111 (2003).
- [8] F. K. Wilhelm, M. J. Storcz, C. H. van der Wal, C. J.
P. M. Hamans, and J. E. Mooij, *Adv. Solid State Phys.*
43, 763 (2003).
- [9] A number of conclusions about the matrix $M(\omega)$ can
be made by using the properties of $M(\omega)$; (i) $M(\omega) =$
 $M(\omega^*)$, (ii) $M(\omega)$ is symmetric for all ω , and (iii) $M(\omega)$
is "causal" in the sense that all of its poles lie on the
lower half of the complex plane ($\text{Im } \omega < 0$).
- [20] A. G. Redfeld, *IBM J. Res. Develop.* 1, 19 (1957).